Energy Storage and Power Management for Typical 4Q-Load

Freek Baalbergen, *Student Member, IEEE*, Pavol Bauer, *Senior Member, IEEE*, and Jan Abraham Ferreira, *Fellow, IEEE*

***Abstract*—Diesel generators in small electricity grids are mostly not used in a very efficient way. The reason for this is twofold. First of all, the efficiency of a diesel generator is dependent on the ratio determined by the average power divided by the peak power of the generator. The smaller this ratio is, the lower the efficiency. Furthermore, some loads can regenerate energy. In small grids, this energy is mostly not needed elsewhere and should be dissipated. A solution solving both problems previously mentioned is using an energy storage device in the system. This storage can be used for peak shaving and storing regenerated energy. This paper focuses on a generator-set with energy storage. Six different power management strategies are discussed. Calculation of the costs shows that adding an energy storage device lowers the cost for all methods. Verification with simulation and experiments has been carried out.**

***Index Terms*—Costs, diesel-driven generators, energy conservation, energy storage, lithium-ion battery, power electronics, supercapacitor.**

I. Introduction

THE DIESEL generator in a small electricity grid is often not used in a very efficient way. The generator has to supply the peak power of the load. The average power of the load can be much smaller. When the generator is not being used at full load, it gets less efficient. Diesel generators are mostly used for only 30% of the full load [1].

Some loads work in all four quadrants of the voltage–current characteristic (4Q-load). These loads act both as a consumer and as a generator. If such a load is being used in a large grid, the generated energy will immediately be used by one of the other loads. However, in small isolated grids, often a diesel driven generator is used as their main power supply. These small grids cannot accept the regenerated power.

For peak power shaving, using a Variable Speed Constant Frequency (VSCF) generator is an option [1]. However, no regenerated energy can be recovered with such a generator.

Manuscript received June 12, 2008; revised September 17, 2008. First published January 19, 2009; current version published April 29, 2009. This work was supported in part by Epyon BV, in part by Exendis BV, and in part by SenterNovem.

F. Baalbergen was with the Department of Electrical Energy Conversion, Faculty of Electrical Engineering, Mathematics and Computer Science, Delft University of Technology, 2628 Delft, The Netherlands. He is now with the Department of High Voltage Components and Power Systems, Delft University of Technology, 2628 Delft, The Netherlands (e-mail: j.f.baalbergen@tudelft.nl).

P. Bauer and J. A. Ferreira are with the Department of Electrical Energy Conversion, Faculty of Electrical Engineering, Mathematics and Computer Science, Delft University of Technology, 2628 Delft, The Netherlands (e-mail: p.bauer@tudelft.nl; j.a.ferreira@tudelft.nl).

Color versions of one or more of the figures in this paper are available online at http://ieeexplore.ieee.org.

Digital Object Identifier 10.1109/TIE.2009.2012416

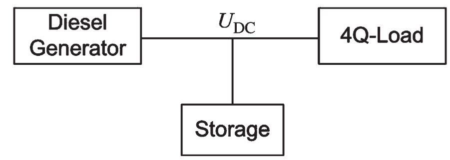

Fig. 1. Diesel generator with energy storage for 4Q-load.

A solution solving both problems previously mentioned is to incorporate an energy storage device in the system. This storage device can be used for peak shaving and storing regenerated energy. The diesel driven generator can be both: a constant speed generator or a VSCF generator. Fig. 1 shows the basic components of such a system.

Different systems are made where an energy storage should increase the efficiency of a system [2]. The most well-known example is the Toyota Prius hybrid car. Research is going on for hybrid electric and electric vehicles [3]–[7]. Elevator systems can also be extended with an energy storage [8]. The same holds for a Rubber-Tyred Gantry crane [9]. In renewable energy systems, storages get also many attention [10]–[15]. Hybrid approaches of different storage systems, as compressed air and supercapacitors, are also under investigation [16]. Research can also be focused on storage solutions for special generators [17]–[19] or the influence of the place of the storage in the system [20]. The converters in such systems are also a topic under investigation [21]–[23].

The aforementioned papers show that there is high attention for energy storage systems in hybrid systems. This paper distinguishes itself from these papers in the fact that the described research is focused on finding general design rules and Power Management Strategies (PMSs). Six strategies are described and compared based on a typical system.

A. Problem Description

Fig. 1 shows the three main blocks of the system. With this hybrid system, three requirements should be achieved.

1) Energy should be saved: the system should use less energy than an approach without energy storage. In the most favorable case no regenerated energy is dissipated.
2) The cost to use this system should be lower or the same as a generator system without energy storage (energy savings should be taken into account).
3) When more loads are connected to the generator, these loads should be controlled independently of each other.

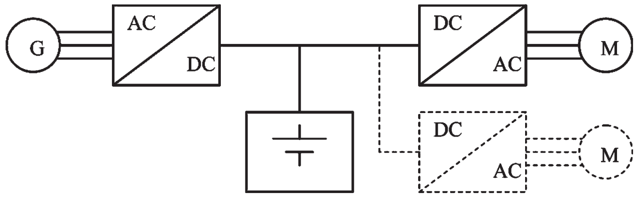

Fig. 2. System topology for generator with Li-ion HP battery.

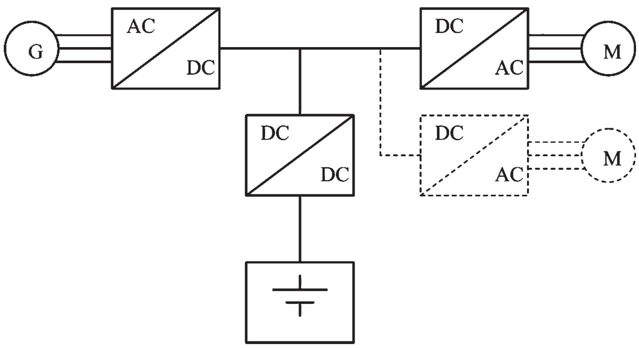

Fig. 3. System topology for generator with supercapacitor.

The problem is to find a PMS meeting these requirements, to determine the size of the energy storage and generator, to determine the costs and to verify the system with simulation and an experimental setup.

In this paper, six different PMSs are investigated, each implying a certain size for the generator and energy storage. The most promising PMS is selected. The selection criteria are the following: energy saving and cost. To compare the energy saving two figures of merit are defined and calculated for each PMS for a typical system. To compare the cost, the cost per cycle for a typical system with the six PMSs is determined.

For the energy storage two different types were compared in a theoretical study. These storages are the following: the lithium-ion High-Power battery and the supercapacitor. These two systems are compared during the cost calculation based on operational costs.

The technical optimum for the size of the generator and energy storage is also investigated.

The system is verified by means of simulation and an experimental setup.

B. System Topology

Because the motors should be controlled independently, only system configurations with separate motor drives are feasible. Two storage elements are investigated: the Li-ion HP battery and the supercapacitor.

The voltage of the Li-ion HP battery varies only a little with the state of charge [24]. Fig. 2 shows the most feasible topology for a system using Li-ion HP battery. The Li-ion HP should be sized so that the depth of discharge (DOD) stays low, so it should be discharged only a little bit.

The voltage of the supercapacitor changes significantly with the state of charge [25]. Fig. 3 shows the most feasible topology for a system using a supercapacitor. The supercapacitor is connected via a bidirectional dc/dc converter to the dc bus.

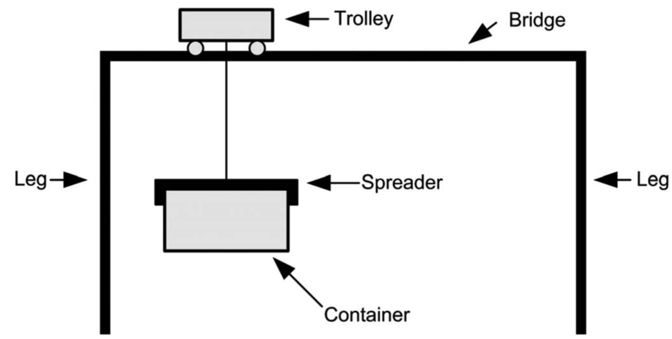

Fig. 4. Typical crane system as used for the case study.

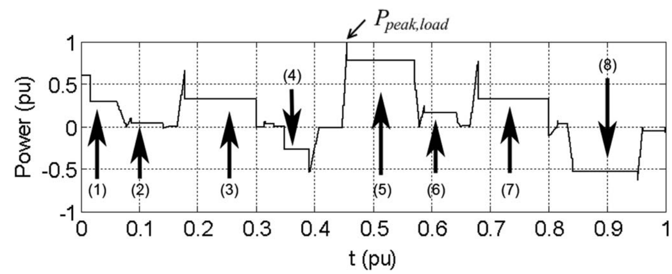

Fig. 5. Load profile used for the crane case study.

II. System for Case Study

The PMSs will be placed in practical condition by a case study: it is a container crane used in the harbor (see Fig. 4). A conventional diesel generator for such a system has an output power range of 30 kVA to 2 MVA [26]. Adding an energy storage to such a system can result in a reduction of 35% in fuel consumption [9].

The generator set with energy storage will be designed based on the worst case scenario for the system. The power load profile, $p_{\mathrm{load}}(t)$, for this scenario is shown in Fig. 5 where the following subsequent duties can be distinguished:

1) hoisting the empty spreader;
2) moving the trolley without load;
3) moving the crane;
4) lowering the spreader without load;
5) hoisting a container;
6) moving the trolley with a container;
7) moving the crane with a container;
8) lowering the container.

The maximum power required is $P_{\mathrm{peak,load}} = 1.0$ p.u. (see Fig. 5), and the average power required by the load is 0.14 p.u. Furthermore, it is given that the diesel generator has a minimum rated output power of $P_{\mathrm{min,rated,gen}} = 0.33$ p.u. Even by applying a storage, the rated power of the generator must not be smaller than $P_{\mathrm{min,rated,gen}}$ because the diesel generator must be able to supply the drive of the crane alone for moving it unloaded in long distances. For safety reasons, it is required that the system contains a braking resistor. The system should have a lifetime of ten years.

All numbers for the case study will be given in per unit. As already given above, the base quantity for the power is defined as the peak power required by the load $P_{\mathrm{base}} = P_{\mathrm{peak,load}}$. The base quantity for the time is defined as the total time needed

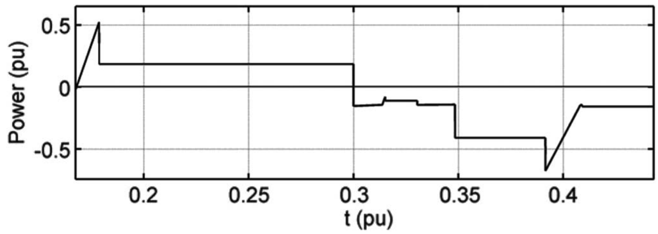

Fig. 6. Detailed part of power profile used for illustrations.

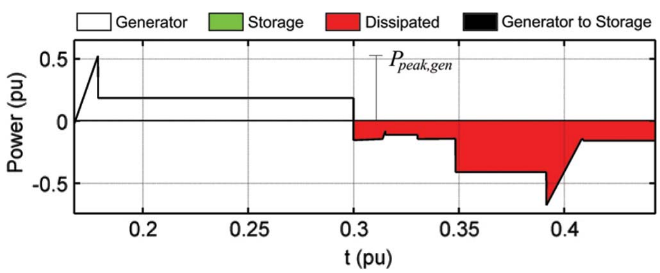

Fig. 7. Illustration of the PMS with OG.

for the profile of Fig. 5, so $t_{\text{base}} = T$. The base quantity for the energy is determined as: $E_{\text{base}} = P_{\text{base}} \cdot t_{\text{base}}$.

III. PMSs

In [27] and [28], different PMSs are defined. In this section, a summary will be given. The power load profile of the case study is quite complex. For that, for each PMS, first the strategy is explained based on a simple section of Fig. 5 (see Fig. 6). This explanation will immediately be followed in all the calculations by the application of the method by using the complex load profile of Fig. 5 in the case study.

A. PMS With OG

In the PMS with Only Generator (OG) the power is fully being supplied by a generator. This system shows no difference with the case applied in practice and is used as a reference. In Fig. 7, an illustration of this method is shown. The size of the generator is marked in this figure.

Applying the load profile for the OG is shown in Fig. 8. In this graph, the power profile for the generator, storage, and braking resistor is given. Because there is no energy storage, the power of this component is zero. If the generator supplies power, this power is positive. Power dissipated in the braking resistor is negative.

The rated peak power of the generator is $P_{\text{rated,peak,gen}} = 1.0$ p.u. The time of the load profile is 1.0 p.u.

B. PMS With PPS

When the PMS with Peak Power Shaving (PPS) is used, the generator supplies most of the power. The storage element supplies only the power peaks needed for short time. More or less, constant power is supplied by the generator. In Fig. 9, an illustration of this method is shown.

Because the storage device has to supply only peak power for small periods, the storage component will be small. Not all regenerated energy can be stored in the storage component because of its small size.

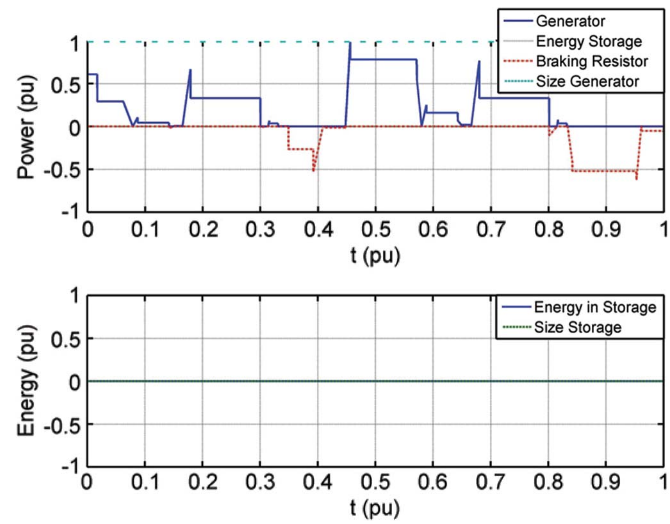

Fig. 8. Power Share and Energy in Storage for the PMS with OG.

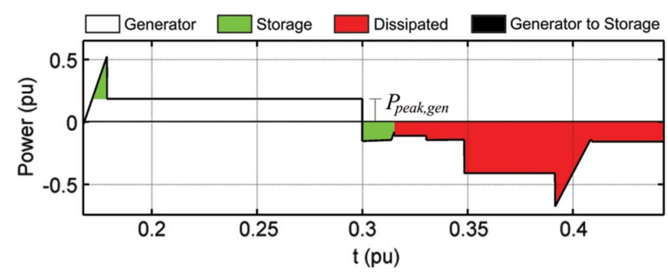

Fig. 9. Illustration of the PMS with PPS.

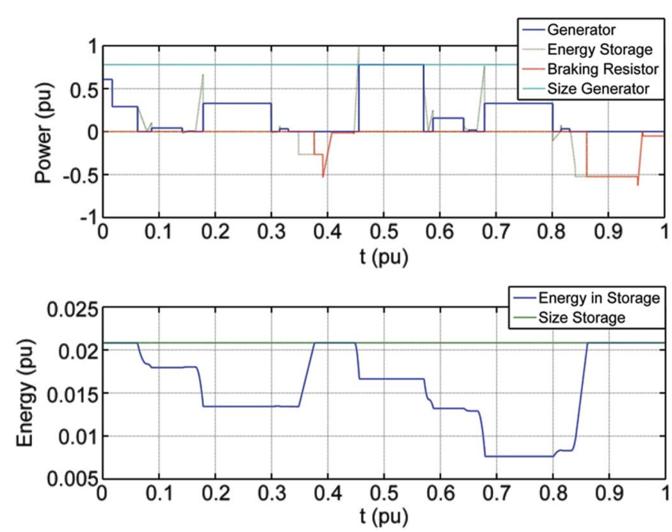

Fig. 10. Power share and energy in storage for the PMS with PPS.

The result for the calculation of the power share for the PPS applied in the case study is shown in Fig. 10. Power drawn from the energy storage is positive, and power stored in the energy storage is negative. At the beginning of power regeneration, first, the storage is charged to its maximum capacity (e.g., around $t = 0.35$ p.u. and $t = 0.83$ p.u).

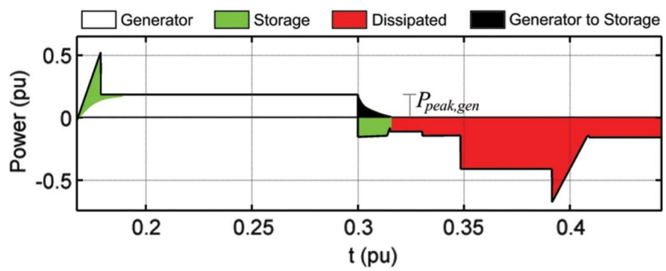

Fig. 11. Illustration of the PMS with DS.

The rated peak power of the generator is $P_{\text{rated,peak,gen}} = 0.78$ p.u. The energy that should be stored in the storage is $E_{\text{peak,stor}} = 0.021$ p.u. The base quantity of the energy is obtained by multiplying the base quantities of the time and the power. An extension to PPS is to incorporate in the algorithm that the generator can be overloaded in a small time. The amount of energy that can be saved will be smaller in that case, and the generator is used less efficiently.

In the lower graph, the time function of the energy in the energy storage is given.

C. PMS With DS

The PMS with Dynamic Solution (DS) is specially designed for use with a VSCF generator. Such a generator cannot react to changes in the output power instantaneously. The energy storage is used to supply the power needed by the load and to absorb the power from the generator in the vicinity of changes. In Fig. 11, an illustration of this method is shown.

It is possible that the storage is not able to capture all the regenerated energy with the DS. This is due to the fact that the storage is used only to supply the power changes.

It is known [1] that transient process in a typical VSCF generator takes $6.7 \cdot 10^{-3}$ p.u. When the generator is overloaded, the VSCF generator will stall [1]. From this, the time constant for raising the power becomes $\tau = (6.7 \cdot 10^{-3})/5 = 1.3 \cdot 10^{-3}$ p.u. Note that these measures are very small.

The result for the calculation of the power share for the DS applied in the case study is shown in Fig. 12. It can be seen that the generator is capable of following some of the changes in load power demand, the slow dynamic behavior that is expected on beforehand is thus not that slow.

The rated peak power of the generator is $P_{\text{rated,peak,gen}} = 0.99$ p.u. The energy that should be stored in the storage element is $E_{\text{peak,stor}} = 0.92 \cdot 10^{-3}$ p.u.

The graph of Fig. 12 does not show clearly the smooth behavior of the generator and that of the storage. For clarification, a detailed view of the first part of the upper graph of Fig. 12 is shown in Fig. 13.

D. PMS With MOO

In the PMS with Max On or Off (MOO), the generator effectively supplies the average power that is needed by the load. For the case study, this average power is $P_{\text{av,load}} = 0.14$ p.u. The generator is switched on, to supply its maximum power $P_{\text{rated,peak,gen}}$, and turned off. The relation among the time

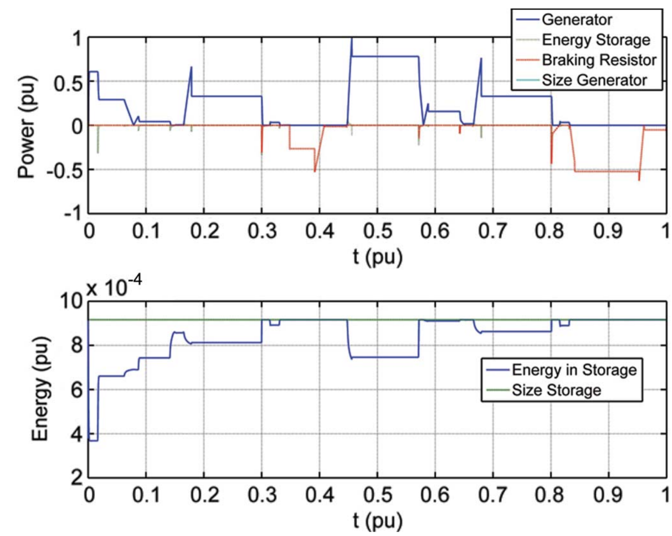

Fig. 12. Power share and energy in storage for the PMS with DS. At $t = 0$, the energy in the storage is $0.92 \cdot 10^{-3}$ p.u.

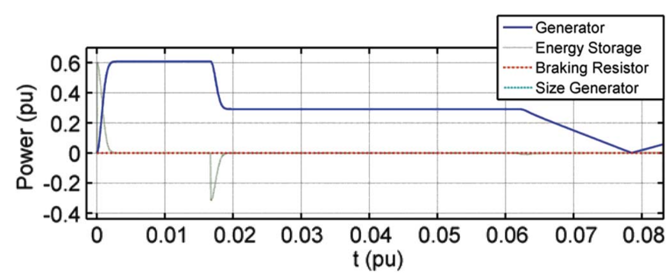

Fig. 13. Detailed part of power share for the PMS with DS.

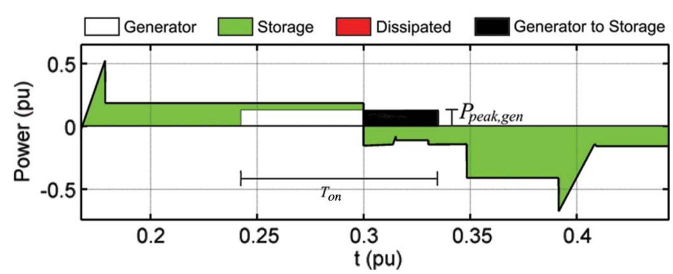

Fig. 14. Illustration of the PMS with MOO.

the generator is on T_{on}, the total time of the load profile T, the average power required by the load $P_{\text{av,load}}$ p.u., and the maximum rated output power of the generator $P_{\text{rated,peak,gen}}$ is

$$P_{\text{av,load}} = \frac{T_{\text{on}}}{T} \cdot P_{\text{rated,peak,gen}}. \quad (1)$$

The generator is dimensioned in such a way that $P_{\text{rated,peak,gen}} \geq P_{\text{av,load}}$.

For a typical cycle, first, the energy is supplied by the energy storage. When the amount of energy in the storage is lower than a certain value, the generator is turned on. The generator stays on until the energy storage is full. In Fig. 14, an illustration of this method is shown. T_{on} is marked in this figure.

Because the on-time of the generator is controlled, this method is well suited for applications where the load profile is not fully known.

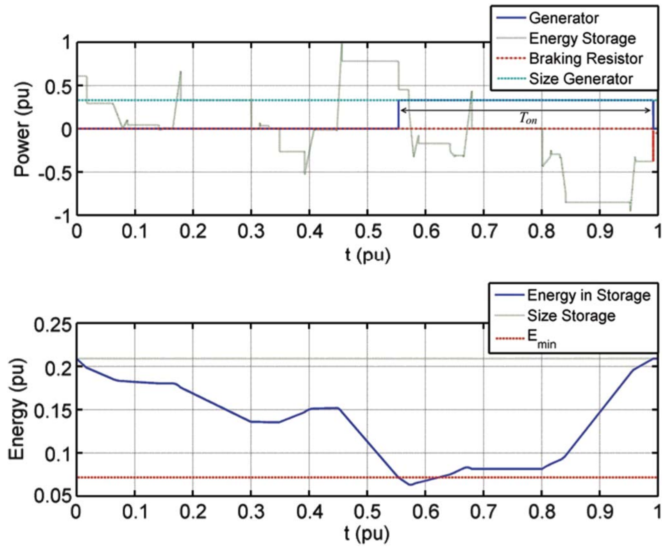

Fig. 15. Power share and energy in storage for the PMS with MOO.

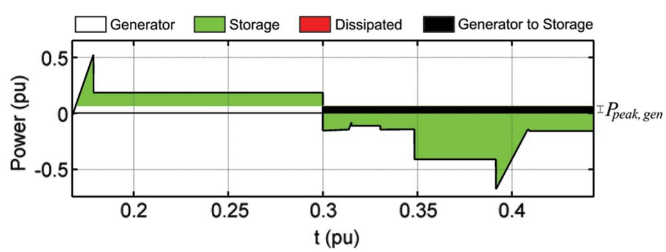

Fig. 16. Illustration of the PMS with AV.

The result for the application of the PMS with MOO for the system in the case study is shown in Fig. 15. The ratio between the on time of the generator and the total time of the power profile is $T_{\rm on}/T = 0.44$.

The maximum rated power of the generator is $P_{\rm rated,peak,gen} = 0.33$ p.u. An extension to MOO is to incorporate in the algorithm that the generator can be overloaded for a small time. The amount of energy that can be saved will be smaller in that case, and the generator is used less efficiently. The peak energy that should be stored in the storage is $E_{\rm peak,stor} = 0.21$ p.u. The minimal energy in the energy storage before the generator is turned on is optimized: $E_{\min} = 0.07$ p.u.

E. PMS With AV

In the PMS with Average Power (AV), the generator continuously supplies the average power needed by the load. For the case study, this average power is $P_{\rm av,load} = 0.14$ p.u. The deviation from the average power will be supplied or absorbed by the storage. An illustration of this method is shown in Fig. 16.

Compared to the MOO, this method is less flexible. With the MOO, the amount of energy supplied by the generator can be controlled by the on time of the generator. With the AV, the average power should be known or estimated on beforehand.

The result for the calculation of the power share for the AV method applied in the case study is shown in Fig. 17.

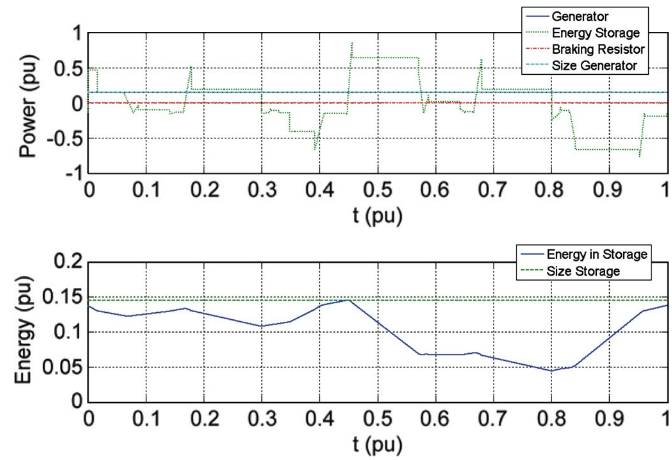

Fig. 17. Power share and energy in storage for the PMS with AV.

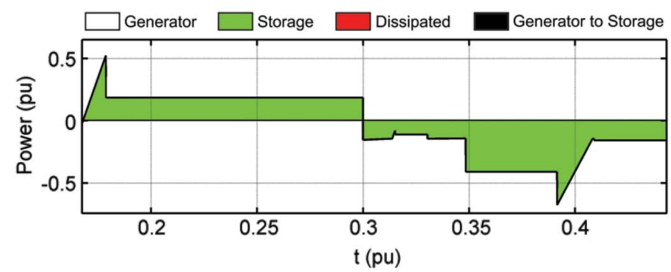

Fig. 18. Illustration of the PMS with OS.

The rated peak power of the generator is $P_{\rm rated,peak,gen} = P_{\rm av,load} = 0.14$ p.u. The peak energy that should be stored in the storage is $E_{\rm peak,stor} = 0.145$.

F. PMS With OS

The PMS with Only Storage (OS) supplies only power from an energy storage device. In Fig. 18, an illustration of this method is shown. The storage can be charged from the grid. Electricity from the grid is less expensive than electricity generated by a diesel generator (comparing [29] and [30]). Further using unbalanced cycles becomes an option. When using unbalanced cycles, the storage is not charged after performing one cycle but after several cycles.

The result for the application of the OS in the case study is shown in Fig. 19. Because there is no generator, the power from the generator is always zero, and no energy is dissipated in the braking resistor.

The peak energy that should be stored in the storage element is $E_{\rm peak,stor} = 0.23$ p.u.

The energy storage becomes never empty. However, after one cycle the storage element contains less energy. The decrease in energy is as follows: $\Delta E_{\rm storage} = 0.14$ p.u. The fact that the energy in the energy storage decreases makes this system not feasible as stand alone system.

IV. Figures of Merit

To compare the merits of the different PMSs for energy savings, two figures of merit are defined. The energy RECovery

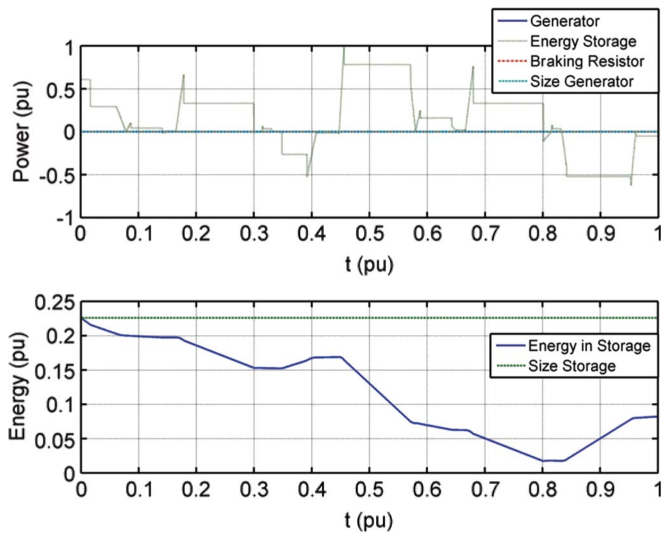

Fig. 19. Power share and energy in storage for the PMS with OS.

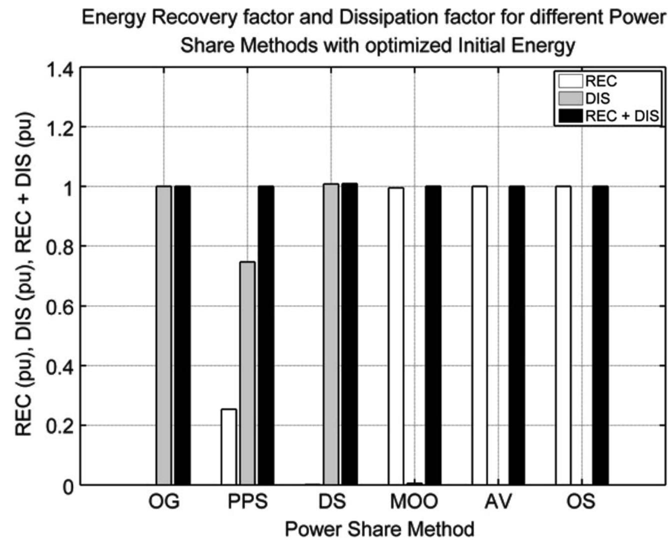

Fig. 20. Energy recovery factor, dissipation factor, and the sum of both for the different PMSs.

factor is the ratio of the total amount of energy recovered from the load and stored in the storage in one cycle ($E_{\text{recovered}}$) divided by the total energy that could have been recovered from the load in one cycle ($E_{\text{regenerated}}$)

$$REC = \frac{E_{\text{recovered}}}{E_{\text{regenerated}}}. \quad (2)$$

The DISsipation factor is the ratio of the total dissipated energy in one cycle ($E_{\text{dissipated}}$) and the total energy that could have been recovered from the load in one cycle ($E_{\text{regenerated}}$)

$$DIS = \frac{E_{\text{dissipated}}}{E_{\text{regenerated}}}. \quad (3)$$

If $REC + DIS = 1$, the total energy regenerated by the load is partly stored in the storage, and the remaining part is dissipated. If $REC + DIS > 1$, energy coming straight from the generator is dissipated as well. This is a disadvantageous situation.

In Fig. 20, the REC, DIS, and the sum of both are compared for the case study. Looking at the REC, it can be seen that AV and OS capture all the regenerated energy, and no energy is dissipated in these PMSs.

These two methods are closely followed by the MOO. In this method, the REC is slightly lower than one, and some energy is dissipated. No energy flows directly from the generator to the braking resistor ($REC + DIS = 1$). Iteration of the optimization process will optimize the REC and DIS more. This optimization can be done based on $E_{\min}$, which is the energy in the energy storage at the moment the generator is turned on.

In the PPS, the energy storage is not large enough to store all the regenerated energy. Therefore, the REC is low and the DIS is high. However, $REC + DIS = 1$.

The DS has a significantly low REC. This is due to the fact that the capacity of the energy storage is very low. A larger time constant of the generator would lead to a larger storage, and a higher REC. Zooming in at the DS, we will see that $REC + DIS > 1 (REC = 0.003$ and $DIS = 1.003)$. Some power from the generator is directly dissipated. This is due to the fact that the output power of the generator cannot be controlled fast enough down, when less power is needed. If this energy cannot be stored, it has to be dissipated.

In the OG, no energy storage element is present, and no energy can be stored.

V. Costs

A detailed calculation of the costs for the system is given in [31]. In this paper, the general calculation method and general results are outlined.

A. Lifetime

We will first have a look at the lifetime of the *Li-ion HP battery*. In this paper, lifetime means the number of years a storage can be used before it should be replaced. The cycle life is the number of cycles the storage can perform before it is replaced.

The system should have a lifetime of ten years. During this ten years, the system has to perform x cycles. In the case study, these x cycles are given by the number of containers that should be hoist in ten years. For each PMS, it is assumed that one cycle of the crane implies one important discharge cycle. Therefore, it is assumed that the battery will encounter x discharge cycles during its life.

The capacity of the battery decreases with age and number of cycles performed. Therefore, at the end of life (EOL) of the battery, only a part of the initial capacity is left. The percentage of the initial capacity that is left at the end of the lifetime of the battery is given by EOL. We should take this percentage into account when we determine the size of the battery.

The lifetime of a Li-ion HP battery is depended on the DOD, number of cycles, and the age [24]. The dependence of the battery lifetime on the DOD is not linear: A lower DOD means a much longer cycle life [24]. This relation is shown schematically in Fig. 21.

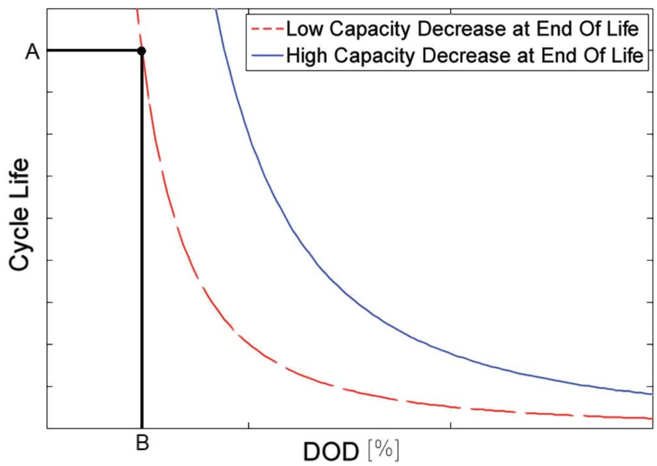

Fig. 21. Dependency cycle life on DOD.

The use of this figure needs some explanation. Assume we want the Li-ion encounters $x = \mathrm{A}$ discharge cycles during its total life. Furthermore, assume that we want to have a low capacity decrease at the EOL corresponding to the red graph in Fig. 21. We see that we can only discharge the battery until $DOD = \mathrm{B}$. Therefore, we only use the part B from the total capacity of the battery.

Because we use only a small part of the total capacity of the battery, it should be oversized. Furthermore, we should take into account the fact that the capacity at the EOL of the battery is lower than at the beginning. The oversize factor for the battery is given by [32], [33]

$$overSize_{\text{Li-ionHP}} = \frac{1}{EOL/100} \cdot \frac{1}{DOD/100}. \quad (4)$$

To make the system most economical, the oversize factor should be as low as possible. Therefore, (4) should be minimized. Calculations for the case study showed that the Li-ion HP battery can best be used until the capacity decreased to 60%, so $EOL = 60\%$. The DOD is should be 3.89%. This implies that the battery should be oversized by a factor 42.8. This means that the Li-ion HP battery should be 42.8 times larger than the peak power that is saved in the battery. The lifetime of a Li-ion battery is generally ten years [34] so the system should met its lifetime criterion.

We will now have a look at the lifetime of the *supercapacitor*. The cycle life of the capacitor is dependent on temperature and voltage and not on the DOD [35]. It is known that a supercapacitor can have more than 500 000 cycles [34], [35]. It is assumed that the x cycles are no problem for the supercapacitor The lifetime of the supercapacitor is ten years [34].

It is known from [35] that at the EOL, the capacity of the supercapacitor is decreased to $EOL = 70\%$. This should be taken into account for the oversizing of the supercapacitor.

The voltage of the supercapacitor drops with the energy stored in it ($E = 1/2C \cdot V^2$). To keep the voltage in an allowable range for the dc/dc converter, from [25], it is known that the supercapacitor should be oversized with a factor 1.56.

TABLE I
DATA FOR COST CALCULATION

Parameter	Data
Price fuel	1.00 [Euro/l] [30]
Price electricity	0.10 [Euro/kWh] [29]
Price Li-ion HP	2000 [Euro/kWh]
Price super capacitor	45000 [Euro/kWh] [34]
Price generator	$59 \cdot 10^3 \cdot P_{rated,peak,gen} + 4676$ [Euro]
Price power electronics	75 [Euro/kW]
Caloric value diesel	35700 [kJ/l] [36]
Fuel efficiency generator	43 % [37]

The total oversize factor for the supercapacitor is thus (based on [32] and [33])

$$overSize_{\text{supercapacitor}} = 1.56 \cdot \frac{1}{EOL} = 2.23. \quad (5)$$

This is remarkably lower than the oversize factor of the Li-ion HP.

B. *Method for Calculation of the Costs*

The total costs per cycle of the hybrid generator can be calculated with

$$Cost_{\text{total}} = Cost_{\text{stor}} + Cost_{\text{gen}} + Cost_{\text{PE}} + Cost_{\text{fuel}} \quad (6)$$

where $Cost_{\text{stor}}$ is the costs per cycle of the storage, $Cost_{\text{gen}}$ the costs per cycle of the generator, and $Cost_{\text{PE}}$ the costs per cycle of the power electronics. In the following equations, x is the number of cycles in ten years.

The costs per cycle of the storage can be calculated with

$$Cost_{\text{stor}} = (1 + r)\frac{IE_{\text{stor}}}{x} \quad (7)$$

where r is the number of replacements during ten years (ideally zero) and IE_{stor} is the initial expense for the storage element

$$IE_{\text{stor}} = Price_{\text{stor}} \times overSize_{\text{stor}} \times E_{\text{peak,stor}} \quad (8)$$

where $Price_{\text{stor}}$ is the price per energy amount (in joule or kilowatt hour) for the storage.

The costs per cycle of the generator can be calculated with

$$Cost_{\text{gen}} = \frac{IE_{\text{gen}}}{x} \quad (9)$$

where IE_{gen} is the initial expense for the generator. This initial expense can be calculated with the equation in Table I.

The costs per cycle of the power electronics can be calculated with

$$Cost_{\text{PE}} = \frac{IE_{\text{PE}}}{x} \quad (10)$$

where IE_{PE} is the initial expense for the power electronics:

$$IE_{\text{PE}} = Price_{\text{PE}} \times P_{\text{PE}} \quad (11)$$

where $Price_{\text{PE}}$ is the price per amount of power for the power electronics, and P_{PE} is the power that the power electronics

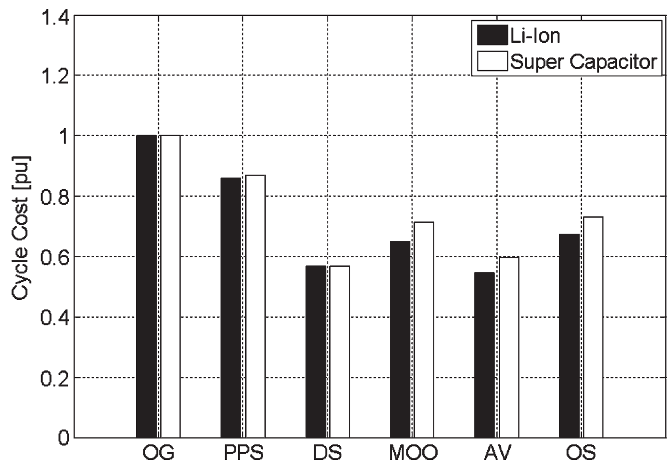

Fig. 22. Comparison for costs for the different PMSs for Li-ion system and supercapacitor system.

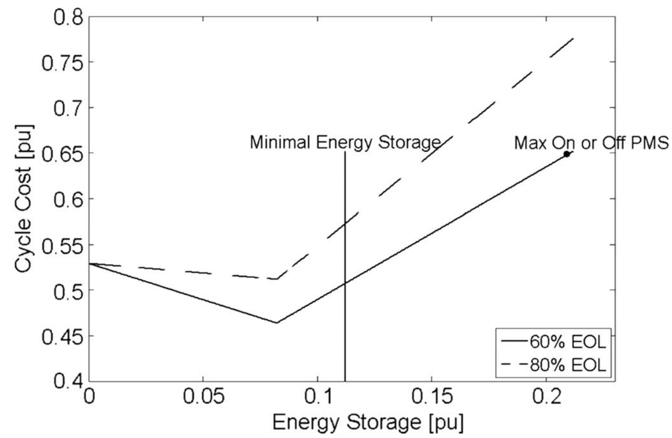

Fig. 23. Cycle costs for different content of energy storage for 0.33-p.u.-rated generator power.

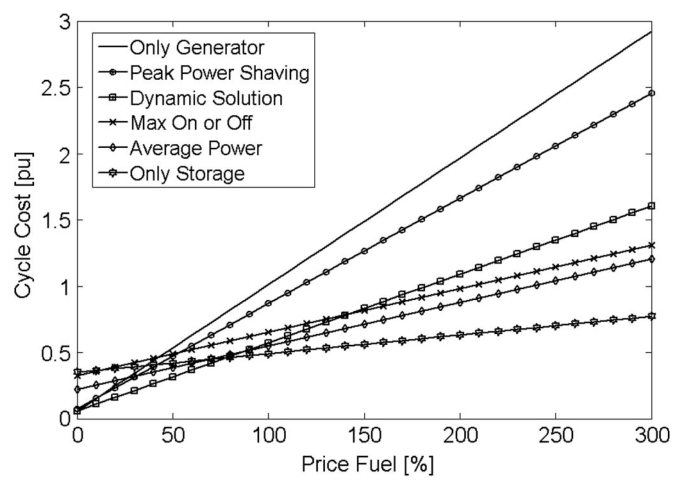

Fig. 24. Sensitivity study: fuel price is changed.

should be able to handle. For the system with Li-ion HP, there is only power electronics for the generators rectifier. In this case, $P_{\mathrm{PE}} = P_{\mathrm{rated,peak,gen}}$. In the case of the supercapacitor, there are power electronics at the generator and at the storage side. In this case, $P_{\mathrm{PE}} = P_{\mathrm{peak,load}}$.

The costs per cycle for the fuel can be calculated with

$$Cost_{\mathrm{fuel}} = fc \times Price_{\mathrm{fuel}} \times P_{\mathrm{av,generator}} \tag{12}$$

where fc is the fuel consumption, and $Price_{\mathrm{fuel}}$ is the fuel price. The fuel consumption is dependent on the use of the generator. For DS, it is assumed, based on the properties of the VSCF generator [1], that the fuel consumption is always one (optimal). For the other methods, based on [38], the following equation is derived:

$$fc = \frac{1}{4} + \frac{3}{4}\frac{P_{\mathrm{av,generator}}}{P_{\mathrm{rated,peak,gen}}}. \tag{13}$$

C. Results for Calculation of the Costs

The aforementioned described method is used to calculate the costs for the system with a Li-ion HP battery that is used until 60% EOL and a system with a supercapacitor. Data used are given in Table I.

In Fig. 22, the costs in per unit are shown for the different PMSs. The costs for the OG is chosen 1 p.u. The battery is oversized with the optimal factor (42.8). It is not necessary to replace the storage. For the OS, it is assumed that the power electronics is dimensioned for 1 p.u. Furthermore, it is assumed for this PMS that the energy comes from the grid.

It can be seen that the costs per cycle are higher for the supercapacitor system than for the Li-ion HP system.

The generator is used most optimal if the relative fuel consumption is one. From the calculations, it becomes clear that the PMSs using the generator most optimal (DS, MOO, AV, and OS), have the lowest costs. The AV has the lowest costs of all.

The costs depends linearly on the size of the generator [31]. Optimizing the costs with respect to the generator power is thus lowering this power.

The solid line in Fig. 23 shows the cycle costs for different sizes of the Li-ion HP battery. The generator power is 0.33 p.u., and the relative fuel consumption is one. The minimal energy content of the energy storage is marked. This minimal energy content of the storage is the first point where the conditions of the boundaries are met. There is an optimum for the energy content of the energy storage. This optimum is, however, for an energy content that is lower than the minimal required. However, it becomes clear that the energy storage for the MOO method can be optimized. It can be shown that the energy storage can be optimized if an energy content of $0.21\text{–}0.07 = 0.14$ p.u. is taken. The costs per cycle would be 0.55 p.u.

The dashed line in Fig. 23 shows the costs for a system used at up to 80% EOL. The same effect is observed as for the 60% EOL line. The costs for a Li-ion HP used up to 80% EOL are higher.

D. Sensitivity Study

In this section, a sensitivity study will be carried out for the costs of a system with Li-ion HP (60% EOL) using the six defined PMSs.

In the figures starting from Figs. 24–27, the costs per cycle are shown for the different PMSs. In the four different

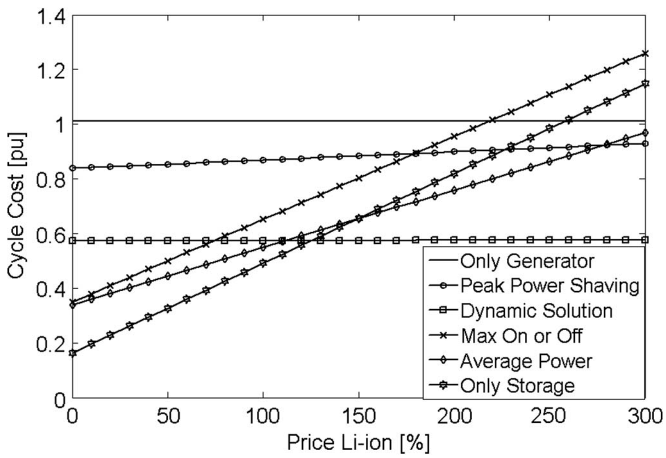

Fig. 25. Sensitivity study: Li-ion price is changed.

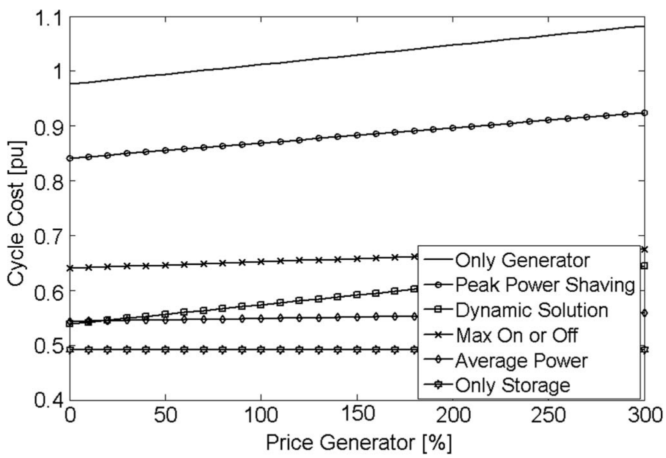

Fig. 26. Sensitivity study: generator price is changed.

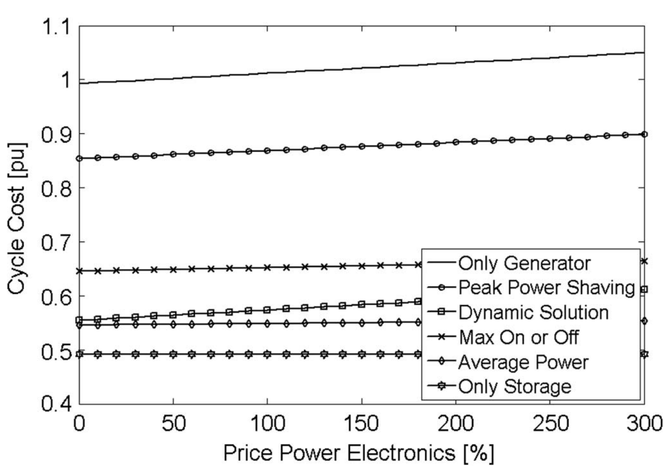

Fig. 27. Sensitivity study: power electronics price is changed.

graphs, the 1) diesel price (Fig. 24), 2) Li-ion price (Fig. 25), 3) generator price (Fig. 26), and 4) power electronic price (Fig. 27) are varied between 0% and 300% of the value used in the calculation of the cost.

From these calculations, it becomes clear that the fuel price is the most sensitive quantity. For the PMSs using a small energy storage (OG, PPS, and DS), it is even the only element that is important from sensitivity point of view. For the OS method, it is assumed that the energy comes from the grid.

For the systems using a larger storage (MOO, AV, and OS), the price of this storage becomes also a sensitive quantity. The larger the energy storage is, the more sensitive the costs become for the price of the storage element.

Based on future trends, the AV and MOO will become more and more advantageous compared to the DS. After an increase of 40% of the fuel price or a decrease of 25% in the Li-ion HP prices, the MOO has an advantage over the DS.

E. Unbalanced Cycles

One of the advantages of using an oversized Li-ion HP battery is the possibility to use unbalanced cycles. When using unbalanced cycles, the energy storage is not charged after one cycle but after for instance ten cycles. This means that after one cycle, the battery is not necessarily charged. In [31], it is shown that using unbalanced cycles becomes too expensive.

VI. Theoretical Discussion

The necessary output power of the generator and the size of the energy storage are determined by the PMS used. For the size of the energy storage, we should also take into account the aging as described in Section V-A. In this section, a more general view of the problem is given. The questions in this section are as follows.

1) What are the possible sizes for the generator and energy storage?
2) Is there a global technical optimum?
3) Is this technical optimum reached by one of the PMSs?

It is assumed that the energy storage is a Li-ion HP battery.

The possible sizes of the generator and battery are limited by the following boundaries.

1) The generator should be able to supply the average power required by the load.
2) The combination of the battery and generator should be able to supply the total energy needed by the load at every time instant.
3) The battery should be able to supply the power peaks required.
4) It makes no sense to have a generator that can supply more power than the required peak load power.

Note that the aforementioned given boundaries hold for an autonomous system.

An illustration of these boundaries is shown in Fig. 28(a). At the x-axis, the size of the generator is given, and at the y-axis, the size of the storage element. The shaded area marks the territory where either a combination of the size of the battery and the size of generator is possible, the numbers of the boundary listed in the four points above.

From the last section, we know that we should oversize the energy storage to meet a specific lifetime of the battery. In Fig. 28(a), a dashed line is shown that illustrates the boundary introduced by the necessary lifetime of the battery. Here, we

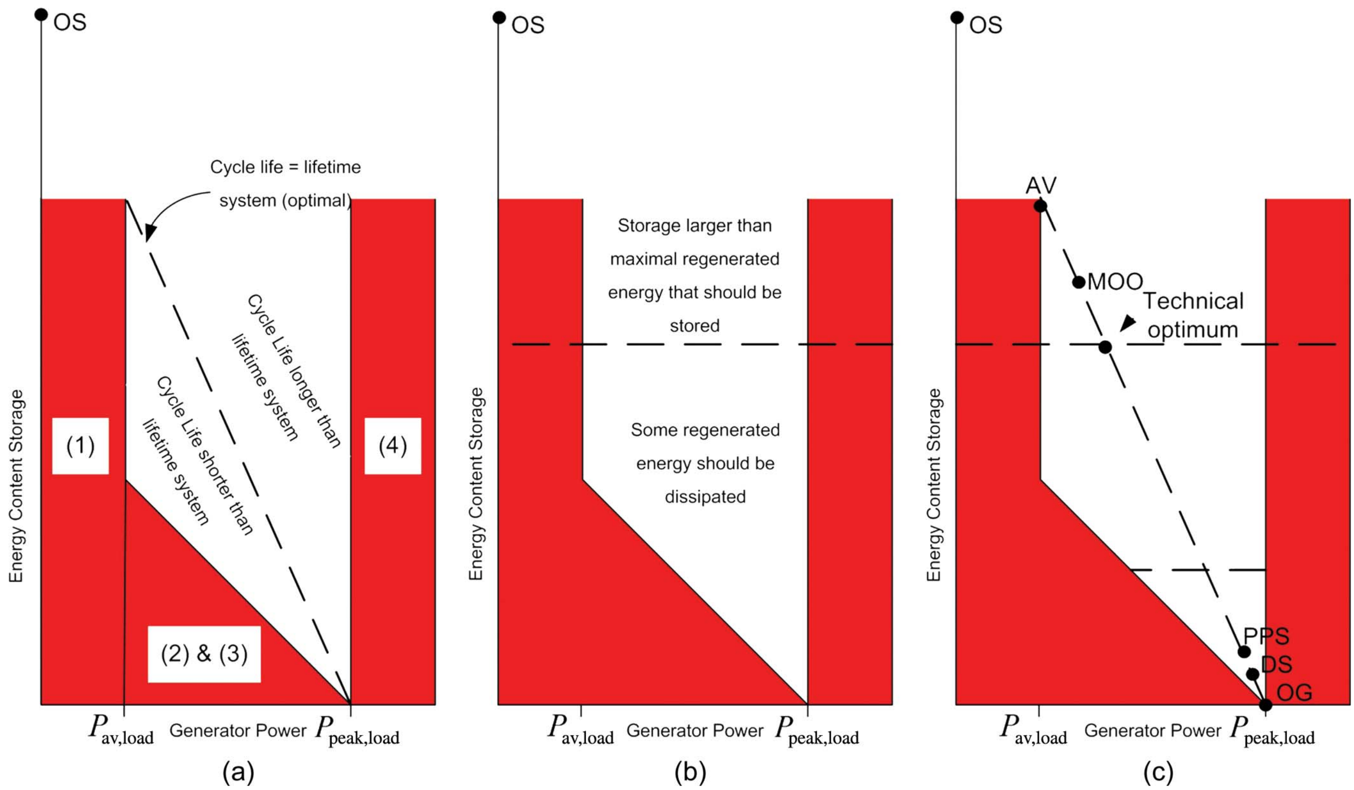

Fig. 28. Sizes of generator and storage.

assume for simplicity a linear relation between the oversizing and the lifetime. When the combination of the size of the generator and battery is below this line, the lifetime will be too short. It makes, however, also no sense to have a combination that lies above the line: In that case, the lifetime is longer than necessary. The dashed line gives thus an optimum.

Considering energy saving and optimum can also be found. This is when all regenerated energy can be stored in the energy storage. This is given with the horizontal line in [Fig. 28(b)]. When the combination of the sizes of the energy storage and battery are below this line, some energy should be dissipated. When the combination of the sizes of the energy storage and battery are above this line, all regenerated energy can be stored. In the figure, it is taken into account that we have to oversize the battery.

Combining the optimal lines for the lifetime [Fig. 28(a)] and the optimal line for energy savings [Fig. 28(b)] gives a technical optimum. This is shown in Fig. 28(c). Therefore, there is a technical optimum.

In the figure, an illustration is also shown for the points where the defined PMSs would be. Note that although for MOO, AV, and OS $REC = 1$, the points in Fig. 28(c) are above the horizontal line. This is due to the fact that in this figure, we see the size of the storage. This size of the storage is not necessarily the average energy needed.

The defined PMSs are not at the technical optimum. The technical optimum could be reached by extending the MOO method by dimensioning the generator and energy storage as given by the technical optimum and change T_{on}/T according to this. This is not further investigated in this paper.

VII. Verification

All PMSs are verified by simulation, and the MOO, AV, and OS are verified by an experimental setup. The figures of merit and costs calculation show that the MOO is the most promising PMS. In this section, a summary of the simulation and experimental setup will be given. The control algorithm for MOO is shown in Fig. 29. $e_{\text{storage}}(t)$ denotes the time function of the energy stored.

A. Simulation

The electrical model used for simulation is shown in Fig. 30. The generator with power electronics and load are simulated with controllable current sources. For the battery, the simple model of [39] is used. This model is sufficiently accurate, and the parameters can be found in data sheets.

The system of Fig. 30 can be described by the following set of equations:

$$\begin{aligned} i_l(t) &= i_b(t) + i_g(t) \\ u_{\text{DC}}(t) &= E_0 - R_i \cdot i_b(t) \\ p_{\text{storage}}(t) &= u_{\text{DC}}(t) \cdot i_b(t) \\ e_{\text{storage}}(t) &= E_{\text{initial}} - \int p_{\text{storage}}(t)dt \\ i_g(t) &= g\left(t, i_l(t), e_{\text{storage}}(t)\right). \end{aligned} \tag{14}$$

In this set of equations, $i_g(t)$ is determined by the algorithm of Fig. 29. In addition to this set of equations, the current from

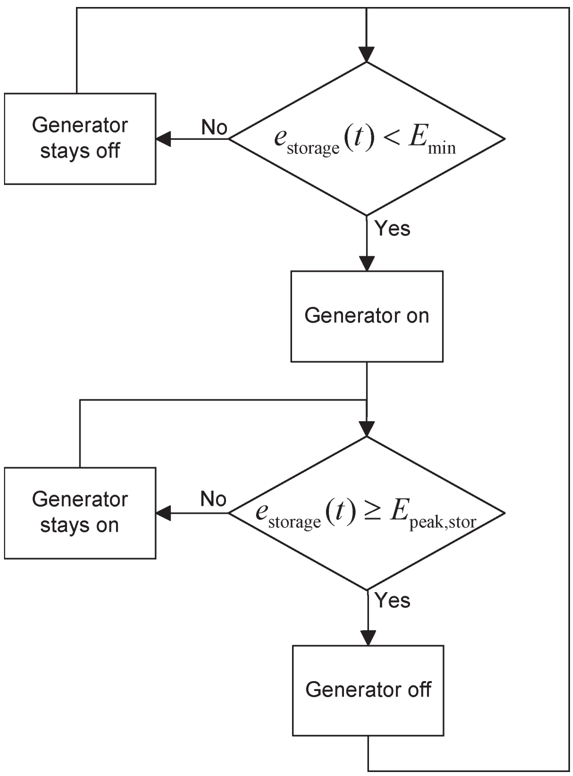

Fig. 29. Control algorithm for MOO.

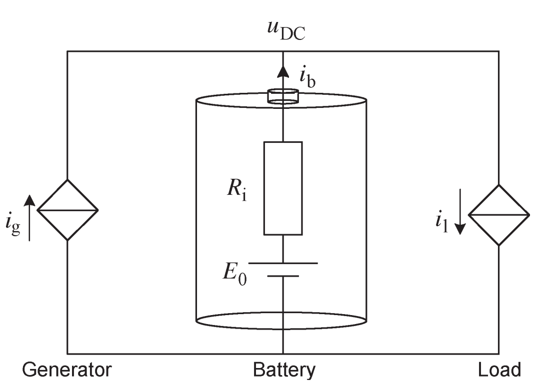

Fig. 30. Electrical model used for simulation.

the breaking resistor can be calculated with

$$\begin{array}{ll} i_{br}(t) = i_l(t), & i_l(t) < 0 \wedge e_{\text{storage}}(t) < E_{\min} \\ i_{br}(t) = 0, & \text{otherwise.} \end{array} \tag{15}$$

The current load profile is calculated on beforehand

$$i_l(t) = \frac{p_{\text{load}}(t)}{U_{\text{DC}}}. \tag{16}$$

If the dc-bus voltage varies, there will be an error. This can be compensated by first running the simulation with the current load profile of (16) for obtaining u_{DC}. From this, the new current load profile can be calculated with

$$i_{l,\text{corrected}}(t) = \frac{U_{\text{DC}}}{U_{\text{DC}} - u_{\text{DC}}(t)} \cdot i_l(t). \tag{17}$$

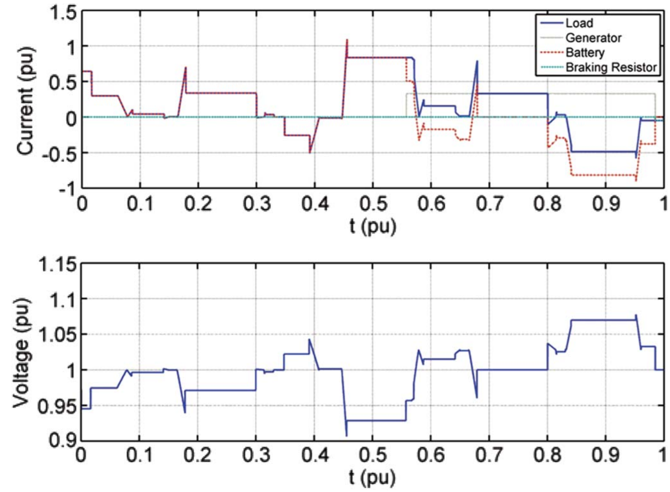

Fig. 31. Results: simulation voltage and currents for MOO.

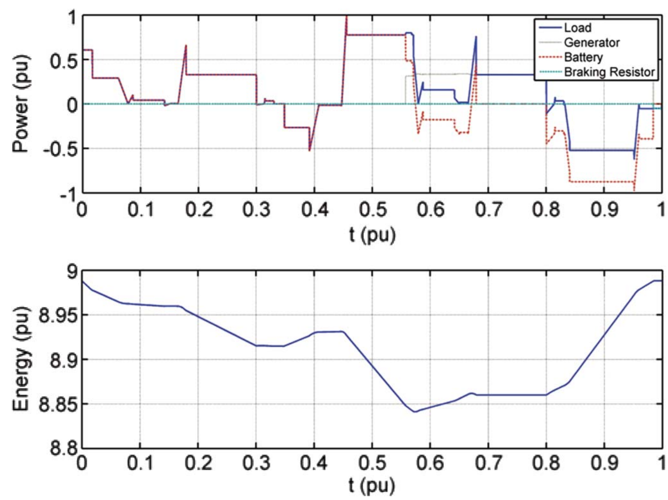

Fig. 32. Results: simulation power and energy for MOO.

The rated peak current of the generator is found with

$$I_{\text{rated,peak,gen}} = \frac{P_{\text{rated,peak,gen}}}{U_{\text{DC}}}. \tag{18}$$

Equation (14) is used to construct a Simulink model. In this model, constrains are also incorporated that: The storage can only be charged or discharged if it is neither empty nor full ($0 < e_{\text{storage}}(t) < E_{\text{peak,stor}}$), or if the storage is full but power is drawn from it ($e_{\text{storage}}(t) = E_{\text{peak,stor}} \wedge p_{\text{load}}(t) - p_{\text{generator}}(t) < 0$), or if the storage is empty but it should be charged ($e_{\text{storage}} = 0 \wedge p_{\text{load}}(t) > 0$).

In this simulation, it is assumed that $R_i = 0.078$ p.u. and the rated voltage of the battery is $E_0 = 1$ p.u. Because MOO is used, sizes of energy storage and generator for this method are used. Based on Section V-A, the energy content from the storage calculated: $E_{\text{peak,stor}} = 42.8 \cdot 0.21 = 8.99$ p.u. The criterion that the generator should be turned on is as follows: $E_{\min} = 8.99 - (0.21 - 0.07)$ p.u., where 0.21 p.u. is the peak energy stored and 0.07 p.u. is the minimal energy stored.

In Fig. 31, the currents and the dc-bus voltage are shown. It can be seen that only a little energy should be dissipated

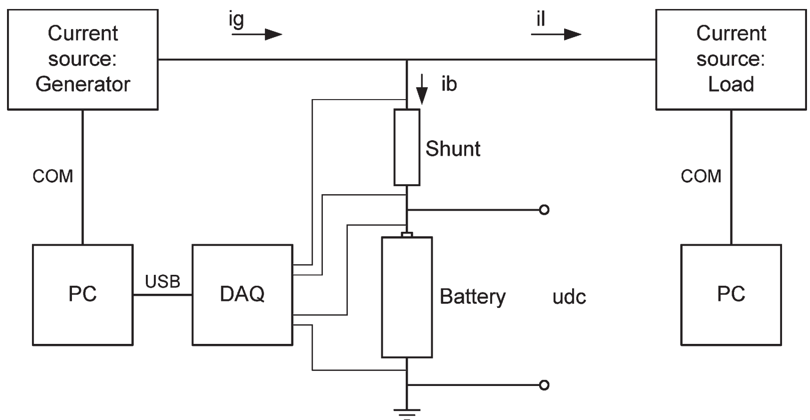

Fig. 33. Experimental setup.

by an braking resistor ($7.3 \cdot 10^{-8}$ p.u.). This is only seen by calculation. The amount of energy that should be dissipated is small and can be found at the end of the cycle. The ripple in the voltage has a maximum value of 7.8% in positive direction and 9.0% in negative direction, which is high.

In Fig. 32, the powers and the energy in the battery are shown. It can be seen that the battery is fully charged at the end of a cycle and that although the current from the generator is switched only between two values, the power varies with the dc voltage. The generator is on for 0.43 p.u. It was calculated that the generator should be on for 0.44 p.u.. The power profile is not as smooth as it was calculated. Furthermore, the change of $e_{\mathrm{storage}}(t)$ obtained by calculation (Fig. 32) and by simulation (Fig. 15) differ only due to the voltage ripple. The control algorithm seems to work properly.

B. Experimental Setup

For the experimental setup, two battery testers from Epyon are used. These testers are sufficiently accurate for this verification. The setup simulates a scaled model. The scheme of the setup is shown in Fig. 33.

One battery tester simulates the load. This battery tester is controlled via a PC and software developed by Epyon to supply the needed current profile. This current profile is calculated from the power load profile and corrected for the ripple on the dc bus

$$i_l = \frac{E_0}{E_0 - R_i \cdot i_b(t)} \cdot \frac{p_{\mathrm{load}}(t)}{E_0} \tag{19}$$

where $R_i = 0.046\ \Omega$ during discharging and $R_i = 0.051\ \Omega$ during charging. This current is also scaled down properly and corrected for a calibration error. Note that the voltage and current are both scaled appropriated related to each other. For the internal resistance, we are dependent on the available energy storages. This internal resistance does not scale with the same factor as voltage and current. Therefore, the experimental setup is mainly to test the algorithm.

The current from the battery is measured via a shunt (60 mV for 6 A) and the voltage of the battery via a $1:11$ resistance divider (10 and 100 kΩ) and measured by a data acquisition card (NI USB-6251). Based on these measurements, LabView

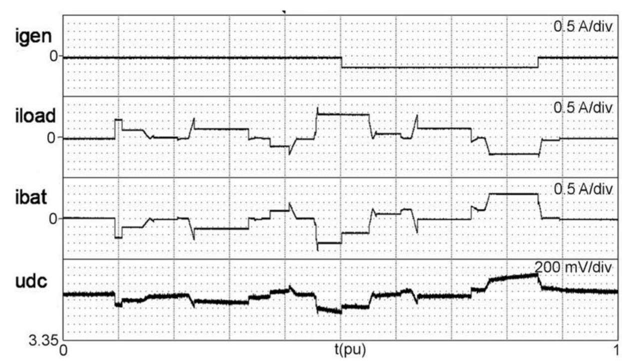

Fig. 34. Currents and dc-bus voltage for MOO.

controls the battery charger simulating the generator. The control signals are sent via the serial port. The PC used to control the “generator” and “load” is the same.

For the experiments, a battery of the manufacturer BMZ is used, type: 1S1P US-18650 VT1. This battery will behave the same as the cells suggested in the case study.

The measurements are done with a Yokogawa DL 1740 digital oscilloscope. The Xviewer software is used to process the data. The currents in the system (igen, iload and ibat) are observed via Tektronix current probes.

Furthermore, the DC-bus voltage (udc) is measured via an $1:10$ probe. At the oscilloscope, the bandwidth is limited to 20 MHz.

The control algorithm of the MOO is implemented in LabView with a small change. The generator is turned on when $e_{\mathrm{storage}}(t)$ drops down at $E_{\min}(e_{\mathrm{storage}}(t) = E_{\min})$ and turned off when $e_{\mathrm{storage}}(t)$ increases up to $E_{\mathrm{peak,stor}}(e_{\mathrm{storage}}(t) = E_{\mathrm{peak,stor}})$.

In Fig. 34, the currents and voltages are shown. A positive current means that the element takes current and a negative current that the element supplies current. The maximal ripple in the voltage is 3.5%. The generator is on for 0.44 p.u.

In Fig. 35, the power from the battery and the energy in the battery are shown. The power from the battery is calculated by multiplying udc with ibat. The energy from the battery is obtained by taking the integral from this power.

The control algorithm seems to work properly. A detailed comparison is difficult to make between the results from the

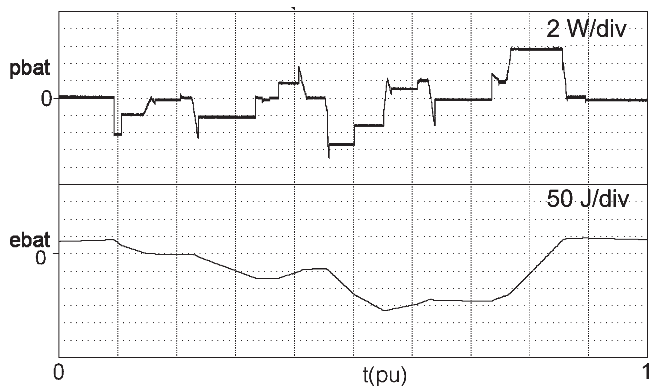

Fig. 35. Power from and energy in battery for MOO.

simulation and the experimental setup. This is because the simulation is based on a model using nonscaled parameters, and the experimental setup is based on a scaled experimental setup. Generally, it can be said that the behavior of the simulation and the experimental setup is comparable.

VIII. Conclusion

Six different PMSs were defined: the OG, PPS, DS, MOO, AV, and OS methods.

Based on energy savings point of view, the MOO, AV, and OS methods are a good choice. The AV and OS methods, however, does not meet the requirement that the generator should have a minimal power of 0.33 p.u.

An important observation that can be made from the calculation of the costs is that adding a storage element to a generator system for a typical crane system lowers the overall costs.

A system based on a Li-ion HP (60% EOL) has lower costs per cycle figure than a system based on supercapacitors. This battery used until 60% EOL leads to lower costs than used until 80% EOL.

The OS, AV, MOO, and DS have the lowest costs per cycle figure. The OS methods, however, only makes sense when used with unbalanced cycles. This, however, is too expensive.

The fuel prices and the storage prices are the most sensitive. Based on future trends, the AV and MOO methods will become more and more advantageous compared to the DS. After an increase of 40% of the fuel price or a decrease of 25% in the Li-ion HP prices, the MOO method is advantageous over the DS.

Looking at cost issues, the MOO and the AV methods are the best choice. Combining this with the energy savings issues, the MOO method is chosen.

Theoretically, a technical optimum is derived. It is shown than none of the defined strategies reaches this optimum. This optimum could, however, be reached by modification of the MOO method.

The MOO method is successfully simulated and tested with an experimental setup.

Acknowledgment

The authors would like to thank C. Bouman (cbouman@epyon.nl) and E. Raaijen (e.raaijen@exendis.com) for their valuable comments. The case study is provided by Epyon BV and Exendis BV, two companies working on practical energy storage systems.

References

[1] J. Leuchter, P. Bauer, V. Rerucha, and V. Hajek, "Dynamic behaviour modeling and verification of advanced electrical-generator set concept," *IEEE Trans. Ind. Electron.*, vol. 56, no. 1, pp. 266–279, Jan. 2008.

[2] R. K. Járdán, I. Nagy, and E. Masada, "Power quality conditioning in a system developed for utilizing waste energies," in *Proc. Annu. Meeting IEE Jpn.*, 2006, pp. 259–260.

[3] K. T. Chau, C. C. Chan, and C. Liu, "Overview of permanent-magnet brushless drives for electric and hybrid electric vehicles," *IEEE Trans. Ind. Electron.*, vol. 55, no. 6, pp. 2246–2257, Jun. 2008.

[4] A. Emadi, Y. J. Lee, and K. Rajashekara, "Power electronics and motor drives in electric, hybrid electric, and plug-in hybrid electric vehicles," *IEEE Trans. Ind. Electron.*, vol. 55, no. 6, pp. 2237–2245, Jun. 2008.

[5] S. M. Lukic, J. Cao, R. C. Bansal, F. Rodriguez, and A. Emadi, "Energy storage systems for automotive applications," *IEEE Trans. Ind. Electron.*, vol. 55, no. 6, pp. 2258–2267, Jun. 2008.

[6] J. Moreno, M. E. Ortuzar, and J. W. Dixon, "Energy-management system for a hybrid electric vehicle, using ultracapacitors and neural networks," *IEEE Trans. Ind. Electron.*, vol. 53, no. 2, pp. 614–623, Apr. 2006.

[7] M. Ortuzar, J. Moreno, and J. Dixon, "Ultracapacitor-based auxiliary energy system for an electric vehicle: Implementation and evaluation," *IEEE Trans. Ind. Electron.*, vol. 54, no. 4, pp. 2147–2156, Aug. 2007.

[8] A. Rufer and P. Barrade, "A supercapacitor-based energy-storage system for elevators with soft commutated interface," *IEEE Trans. Ind. Electron.*, vol. 38, no. 5, pp. 1151–1159, Sep./Oct. 2002.

[9] S. Kim and S. Sul, "Control of rubber tyred gantry crane with energy storage based on supercapacitor," *IEEE Trans. Power Electron.*, vol. 21, no. 5, pp. 1420–1427, Sep. 2006.

[10] R. Cardenas, R. Pena, M. Perez, J. Clare, G. Asher, and F. Vargas, "Vector control of front-end converters for variable-speed wind-diesel systems," *IEEE Trans. Power Electron.*, vol. 54, no. 4, pp. 1127–1136, Jun. 2006.

[11] G. O. Cimuca, C. Saudemont, B. Robyns, and M. M. Radulescu, "Control and performance evaluation of a flywheel energy-storage system associated to a variable-speed wind generator," *IEEE Trans. Power Electron.*, vol. 53, no. 4, pp. 1074–1085, Aug. 2006.

[12] J. M. Carrasco, L. G. Franquelo, J. T. Bialasiewicz, E. Galvan, R. C. P. Guisado, M. A. M. Prats, J. I. Leon, and N. Moreno-Alfonso, "Power-electronic systems for the grid integration of renewable energy sources," *IEEE Trans. Power Electron.*, vol. 53, no. 4, pp. 1002–1016, Jun. 2006.

[13] Z. Jiang and R. Dougal, "A compact digitally controlled fuel cell/battery hybrid power source," *IEEE Trans. Ind. Electron.*, vol. 53, no. 4, pp. 1094–1104, Jun. 2006.

[14] S.-K. Kim, J.-H. Jeon, C.-H. Cho, J.-B. Ahn, and S.-H. Kwon, "Dynamic modeling and control of a grid-connected hybrid generation system with versatile power transfer," *IEEE Trans. Ind. Electron.*, vol. 55, no. 4, pp. 1677–1688, Apr. 2008.

[15] P. Thounthong, S. Rael, and B. Davat, "Control strategy of fuel cell and supercapacitors association for a distributed generation system," *IEEE Trans. Ind. Electron.*, vol. 54, no. 6, pp. 3225–3233, Dec. 2007.

[16] A. R. S. Lemofouet, "A hybrid energy storage system based on compressed air and supercapacitors with maximum efficiency point tracking (MEPT)," *IEEE Trans. Power Electron.*, vol. 53, no. 4, pp. 1105–1115, Aug. 2006.

[17] J. Wang, W. Wang, G. W. Jewell, and D. Howe, "Design of a miniature permanent-magnet generator and energy storage system," *IEEE Trans. Ind. Electron.*, vol. 52, no. 5, pp. 1383–1390, Oct. 2005.

[18] R. K. Jardan and I. Nagy, "Synchronous machine-turbine drive system with indirect speed control," in *Proc. IEEE Int. Elect. Mach. Drives Conf.*, 2003, pp. 1144–1150.

[19] R. K. Jardan, I. Nagy, and Z. Varga, "Special features of ultrahigh-speed induction generators applied in the utilization of renewable energy sources," in *Proc. SPEEDAM*, 2008, pp. 1439–1444.

[20] M. T. Tsai, C. E. Lin, W. I. Tsai, and C. L. Huang, "Design and implementation of a demand-side multifunction battery energy storage system," *IEEE Trans. Ind. Electron.*, vol. 42, no. 6, pp. 642–652, Dec. 1995.

[21] J. Hamar and I. Nagy, "Control features of dual-channel dc–dc converters," *IEEE Trans. Ind. Electron.*, vol. 49, no. 6, pp. 1293–1305, Dec. 2002.

[22] O. Dranga, B. Buti, and I. Nagy, "Stability analysis of a feedback controlled resonant dc–dc converter," *IEEE Trans. Ind. Electron.*, vol. 50, no. 1, pp. 141–152, Feb. 2003.

[23] J. Hamar, B. Buti, and I. Nagy, "Dual channel resonant dc–dc converter family," *EPE J.*, vol. 17, no. 3, pp. 5–15, 2007.

[24] D. Linden and T. Reddy, *Handbook of Batteries*, 3rd ed. New York: McGraw-Hill, 2002.

[25] M. Ehsani, Y. Gao, S. Gay, and A. Emadi, *Modern Electric, Hybridelectric, and Fuel Cell Vehicles: Fundamentals, Theory, and Design*, 1st ed. Boca Raton, FL: CRC Press, 2005.

[26] Portek, *Portek Cranecomponents & Spares Brochure*. (accessed date: 2008, January 17). (in Dutch). [Online]. Available: http://www.portek.com/brochures/spare%20brochure.pdf

[27] J. F. Baalbergen and P. Bauer, "Survey of power management strategies for generator-set with energy storage," in *Proc. PCIM Conf.*, 2008, pp. 1–6.

[28] J. F. Baalbergen and P. Bauer, "Power management strategies for generator-set with energy storage for 4q-load," in *Proc. 39th IEEE PESC*, 2008, pp. 3901–3906.

[29] Nuon, *energietarieven elektriciteit*. (accessed date: 2007, September 26). (in Dutch). [Online]. Available: http://www.nuon.nl

[30] Shell, *historisch prijzenoverzicht*. (accessed date: 2007, June 1). (in Dutch). [Online]. Available: http://www.shell.com

[31] J. F. Baalbergen and P. Bauer, "Cost evaluation of generator-set with energy storage for 4q-load," in *Proc. 13th Int. EPE-PEMC*, 2008, pp. 2193–2200.

[32] *IEEE Recommended Practice for Sizing Lead-Acid Batteries for Stationary Applications*, IEEE Std. 485-1997.

[33] *IEEE Recommended Practice for Sizing Nickel-Cadmium Batteries for Stationary Applications*, IEEE Std. 1115-2000.

[34] M. Piemontesi, "Alternative energy storage systems for ups," in *Proc. Conf. PCIM*, 2006. [CD-ROM].

[35] Nesscap Co., *Nesscap Ultracapacitor Technicalguide*. (accessed date: 2007, May 23). [Online]. Available: http://www.nesscap.com

[36] Emis, *Energy and Milieu Information Centre*. (accessed date: 2007, June 1). (in Dutch). [Online]. Available: http://www.emis.vito.be

[37] L. L. J. Mahon, *Diesel Generator Handbook*. London, U.K.: Butterworth-Heinemann, 1992.

[38] A. Leotta, U. Nocera, and A. Raciti, "Diesel electric power stations," in *Wiley Encyclopedia of Electrical and Electronic Engineering*, vol. 5, 1999, pp. 368–378.

[39] A. Emadi, M. Ehsani, and J. Miller, "Vehicular electric power systems: Land sea, air, and space vehicles," in *Electrical Modeling Techniques for Energy Storage Devices*. New York: Marcel Dekker, 2005.

Freek Baalbergen (S'08) received the B.Sc. and M.Sc. degrees in electrical engineering from Delft University of Technology, Delft, The Netherlands, in 2005 and 2007, respectively, where he is currently working toward the Ph.D. degree in the High Voltage Components and Power Systems Group.

His main topics of interest are energy storage, state estimation, smart grids, and phasor measurements.

Pavol Bauer (SM'07) received the Masters degree in electrical engineering from the Technical University of Kosice, Kosice, Slovakia, in 1985, and the Ph.D. degree from Delft University of Technology, Delft, The Netherlands, in 1995.

He received the title of Professor from the President of the Czech Republic at the Brno University of Technology, Brno, Czech Republic, in 2008. Since 1990, he has been with Delft University of Technology. From 2002 to 2003, he was working part-time with KEMA. He has published over 40 journal and 170 conference papers, is an author or coauthor of five books, and holds international patents. He has organized several tutorials at international conferences. He has worked on many projects for industry and participated in several Leonardo da Vinci EU projects as Project Partner (ELINA, INETELE) and Coordinator (PEMCWebLab.com).

Dr. Bauer is a Senior Member and a Chapter Officer of the IEEE Joint Industry Applications Society, Power Electronics, and Power Engineering Society—Benelux Chapter, a member of the European Power Electronics (EPE)-Power Electronics and Motion Control Council, EPE member, and a member of the international steering committees of numerous conferences.

Jan Abraham Ferreira (F'05) received the B.Sc.Eng. (*cum laude*), M.Sc.Eng. (*cum laude*), and Ph.D. degrees in electrical engineering from Rand Afrikaans University, Johannesburg, South Africa, in 1980, 1982, and 1988, respectively.

In 1981, he was with the Institute of Power Electronics and Electric Drives, Technical University of Aachen, Aachen, Germany, and worked in industry at ESD (Pty) Ltd from 1982 to 1985. From 1986 to 1997, he was with the Faculty of Engineering, Rand Afrikaans University, where he held the Carl and Emily Fuchs Chair of Power Electronics. Since 1998, he has been a Professor with Delft University of Technology, Delft, The Netherlands.

Dr. Ferreira was Chairman of the South African Section of the IEEE, from 1993 to 1994. He is the Founding Chairman of the IEEE Joint Industry Application Society (IAS)/Power Electronics Society (PELS) Benelux Chapter. He served as the TRANSACTIONS Review Chairman of the IEEE IAS Power Electronic Devices and Components Committee and is an Associate Editor of the IEEE TRANSACTIONS ON POWER ELECTRONICS. He was a member of the IEEE PELS AdCom and is currently Treasurer of IEEE PELS. He served as Chairman of the CIGRE SC14 National Committee of the Netherlands and was a member of the Executive Committee of the European Power Electronics Society.